The Interaction of Cyclodextrins with Nucleic Acids. A Study of Secondary Structure in Three Transfer Ribonucleic Acids*

Jerald L. Hoffman† and Robert M. Bock

ABSTRACT: By difference spectroscopy, cycloheptaamylose has been shown to interact with AMP and IMP alone out of six mononucleotides tested. None of the six interacted with cyclohexaamylose. The supposed method of interaction is by inclusion complex formation between the base residue and the cyclodextrin. The main determinant of base specificity appears to be the size of the base relative to the cyclodextrin cavity. Other factors affecting the interaction with cycloheptaamylose are degree and position of phosphorylation, pH, and polymerization of the nucleotide. Interaction of cycloheptaamylose with a base in an environment equivalent to that in a mononucleotide results in a hypochromic change in the ultraviolet absorption of the base. When the base is in a single-stranded stacked conformation, the spectral change is primarily hyperchromic. If the base is in a multistranded helix there is no interaction with cycloheptaamylose. On the basis of the above and other model studies, the difference spectra resulting from interacting cycloheptaamylose with three partially purified tRNAs were analyzed and the following conclusions reached. The adenine (and hypoxanthine) bases of tRNA which are not in helical regions are in single-stranded stacked conformations. The three different tRNAs showed similar degrees of base exposure to cycloheptaamylose only in the presence of magnesium ions, where the degree of exposure was very low. In the absence of magnesium, yeast $tRNA_{II}^{Arg}$ generally showed the greatest base exposure followed by *Escherichia coli* $tRNA^{Phe}$ and then yeast $tRNA_{I}^{Val}$.

The chemical environment of nucleic acid bases changes when going from mononucleotides to single-stranded polymers to double- or triple-stranded helices. Examples of this may be seen in the differential reactivity of tRNA bases depending on their location in helical or nonhelical regions.

The results of studies on tRNA with such reagents as formaldehyde (Penniston and Doty, 1963; Marciello and Zubay, 1964), monoperphthalic acid (Seidel and Cramer, 1965), tritiated water (Englander and Englander, 1965), and kethoxal (Litt and Hancock, 1967) are thought to show that involvement of bases in secondary structure imparts resistance to these reagents.

We proposed to search for substances which, by physical interaction with nucleic acid bases, would produce ultraviolet spectral shifts characteristic of the environment of the bases. The cyclodextrins appeared to be likely compounds for interaction with nucleic acids. This class of compounds results from the digestion of starch by *Bacillus macerans* amylase, yielding macrocyclic oligomers consisting of six or more D-glucosyl residues linked by α-(1–4) bonds (Figure 1). As a result of their cyclic structure, the cyclodextrins form inclusion complexes with a variety of compounds which can fit into their central cavity (see reviews by Thoma and Stewart, 1965, and Cramer and Hettler, 1967).

Since nucleic acid bases are about the same size as many of these compounds, we anticipated inclusion complex formation between cyclodextrins and nucleic acids. Such an interaction should be accompanied by a shift in the ultraviolet spectra of the nucleic acid. Furthermore, since the interaction would supposedly occur by insertion of the base into the cyclodextrin cavity, bases in helices should be resistant to interaction.

Our experimental results, primarily determined using difference spectroscopy, have borne out these anticipations along with the unexpected finding that the interaction is base specific. Having characterized the interaction using model compounds, we have applied the results of the model studies to interpretation of the spectral shifts resulting from interaction of cycloheptaamylose with three partially purified tRNAs.

Materials

The following list gives the sources of commercially obtained materials: cyclohexaamylose (cyclohexane complex) and cycloheptaamylose, Pierce Chemical; mononucleotides, P-L Biochemicals or Schwarz BioResearch; polynucleotides, Miles Laboratories; adenine, adenosine, and *E. coli* DNA, General Biochemicals Inc.; pancreatic ribonuclease, Worthington Biochemicals; Chelex 100, Calbiochem; dual-compartment cuvets, Pyrocell Mfg. Co.; Corey–Pauling–Koltun atomic models, Schwarz BioResearch. Other more common chemicals were generally reagent grade.

In addition, we are grateful to Dr. S. Y. Lee and Dr. F. U. Lichti for a variety of oligonucleotides, to Dr. Joseph Cherayil for samples of yeast arginine and valine tRNA, and to the

* From the Department of Biochemistry and the Laboratory of Molecular Biology, University of Wisconsin, Madison, Wisconsin 53706. *Received August 12, 1969.* Supported by Grant GM 12395 from the National Institutes of Health, Public Health Service. Presented in part at the 51st Annual Federation of American Society of Experimental Biologists Meeting, Chicago, Ill., 1967, Abstract 501.

† Predoctoral Fellow of the National Institutes of Health during this investigation. Data were taken from the thesis submitted by Jerald L. Hoffman in partial fulfillment of the requirements for the degree of Doctor of Philosophy from the University of Wisconsin. Present address: Department of Biochemistry, University of Louisville School of Medicine, Louisville, Ky.

Oak Ridge National Laboratory for a sample of *E. coli* $tRNA^{Phe}$.

Methods

Difference Spectral Measurements. These were performed using a Cary 15 spectrophotometer and a set of dual-compartment cuvets designed by Yankeelov (1963). These are 1-cm rectangular cuvets divided into two compartments by a slotted quartz plate perpendicular to the light path.

At least 0.5 ml of sample solution was pipetted into side one of each cuvet and a precisely equal volume of cyclodextrin solution into side two. With the contents of the cuvets in this configuration, the base line was determined by scanning over the wavelength region of interest. The contents of the two sides of one of the cuvets were mixed by covering the cuvet with Parafilm and repeatedly inverting it. The difference spectrum due to mixing cyclodextrin and sample was then recorded by scanning as before. Maximum sample optical densities of 2.0 ± 0.2 (after mixing) were used in all difference spectral measurements, since slit cutoff occurred at higher concentrations.

Difference spectra were routinely replotted every 5 mμ as follows. If the molar extinction coefficient of the sample was known (enabling spectral determination of the molar base concentration), the difference spectra were plotted as the change in molar extinction coefficient ($\Delta\epsilon$) *vs.* λ.

$$\Delta\epsilon = \frac{OD_{free} - OD_{complex}}{C} = \frac{\Delta OD}{C} \qquad (1)$$

where C = molar base concentration.

If the molar extinction coefficient of the sample was not known, the difference spectra were replotted as the per cent change in optical density relative to the maximum *vs.* λ.

$$\frac{\Delta OD}{OD_{max}} \times 100 = \frac{OD_{free} - OD_{complex}}{OD_{max}} \times 100 \qquad (2)$$

Conventional absorption spectra of each sample were measured apart from difference spectra, again using a Cary 15 spectrophotometer.

Preparation of tRNA Samples. Since the secondary structure of tRNA is dependent on the history of the sample, the three tRNAs used in this study were (prior to spectral measurement) uniformly treated as follows. Samples were desalted on 1.5 × 10 cm columns of Sephadex G-25 followed by passage through 0.8 × 5 cm columns of Chelex 100 to remove traces of divalent cations. These solutions were lyophilized to dryness and redissolved in 0.01 M Tris-HCl buffer at pH 7.4 at sufficiently high concentrations to allow dilution into digestion media or spectral solutions. tRNA so treated showed full acceptor activity.

Ten optical density units of each tRNA was digested with 10 μg of pancreatic ribonuclease in 0.1 ml of 0.01 M Tris buffer at pH 7.4 for 12 hr at room temperature. Four optical density units of each tRNA was hydrolyzed in 0.1 ml of 0.5 M NaOH for 18 hr at room temperature. Aliquots of these digests and of the intact tRNA stock solutions were then diluted into the appropriate buffers for spectral measurements. Where necessary, diluted NaOH digests were adjusted to pH 7.6 with HCl.

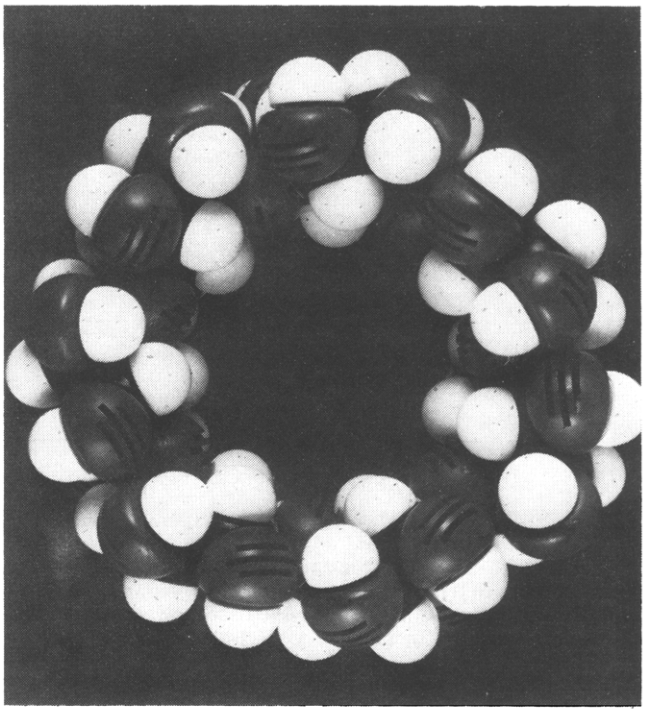

FIGURE 1: Corey–Pauling–Koltun model of cycloheptaamylose. As depicted here, the C_2 and C_3 hydroxyls are facing out from the page and the C_6 hydroxyls are to the back of the molecule. Glycosidic oxygens line the interior of the cavity.

tRNA Melting Curves. These were determined using an electrical resistance heating element built into a Cary 15 rectangular cuvet holder. This apparatus was made by embedding about 45 cm of Nichrome wire in silicone adhesive (Dow Corning Silastic RTV 731) in the spaces left between the cuvet and the sides and bottom of the holder. This heating element was connected to two Variacs in series. With the first set at about 10% of full scale, the second Variac could be used for fine control of cuvet temperature. Temperatures in the cuvet were read by insertion of a type 402 thermistor probe connected to a Telethermometer (both from Yellow Springs Instrument Co.). Heating was done by steps of 1 to 2°, pausing at each increment of Variac setting to allow temperature and optical density equilibration.

Results

Base Specificity of the Interaction. In order to examine the base specificity of possible inclusion complex formation between mononucleotides and cyclodextrins, the difference spectra resulting from mixing cyclohexa- or cycloheptaamylose with the 5′-nucleoside monophosphates AMP, CMP, GMP, UMP, IMP, and dTMP were measured in TSC.[1] At a final concentration of 0.01 M, cyclohexaamylose caused

[1] Abbreviations used are: TSC buffer, 0.01 M Tris + 0.1 M NaCl, to pH 7.6 with HCl; pApA (for example), 5′-*O*-phosphoryladenylyl-[3′,5′]adenosine; poly A:U (for example), the helical complex containing one strand of poly A and one strand of poly U; all polynucleotides used in this work were ribonucleotides.

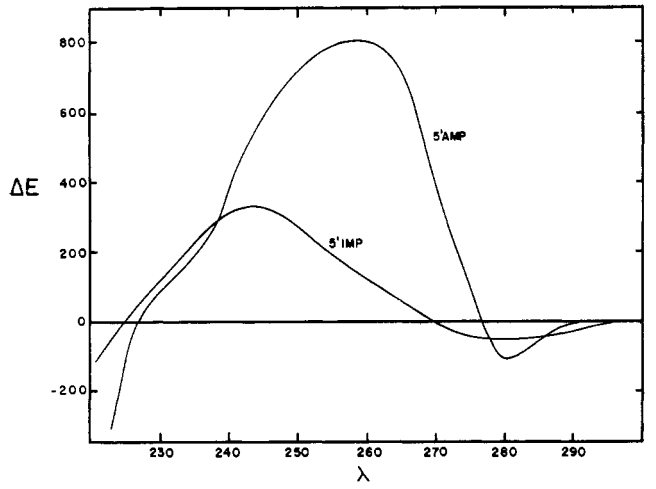

FIGURE 2: Nucleotide difference spectra produced by cycloheptamylose interaction. Difference spectra were produced by 0.01 M cycloheptaamylose in TSC buffer. Maximum optical density units of nucleotide samples in this and other experiments were always within ± 0.2 of being 2.0 after mixing in the cuvets. Exact optical density units were determined apart from difference spectral measurements.

no spectral shift on mixing with any of the six mononucleotides.

However at the same concentration, cycloheptaamylose produced spectral shifts with AMP and IMP (but none of the other mononucleotides) as shown in Figure 2. Keeping in mind that we have defined the difference spectrum as as being equal to the spectrum of the free minus that of the complexed nucleotide, it can be seen that there is a hypochromic shift on complexing, with the largest change occurring at or near the wavelength of maximum absorption of the nucleotide.

The Effect of Nucleoside Formation from Adenine and of Phosphorylation of Adenosine. Figure 3 shows the difference spectra which resulted when adenine, adenosine, 5'-AMP, ADP, or ATP was mixed with cycloheptaamylose. $\Delta\epsilon$ increases in the order adenine, adenosine, ADP, ATP, AMP.

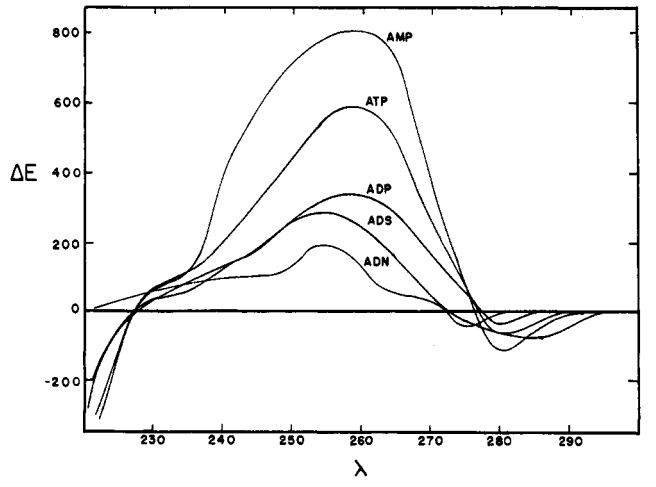

FIGURE 3: The interaction of adenine, adenosine, AMP, ADP, and ATP with cycloheptaamylose: TSC buffer, 0.01 M in cycloheptaamylose; ADN, adenine; ADS, adenosine.

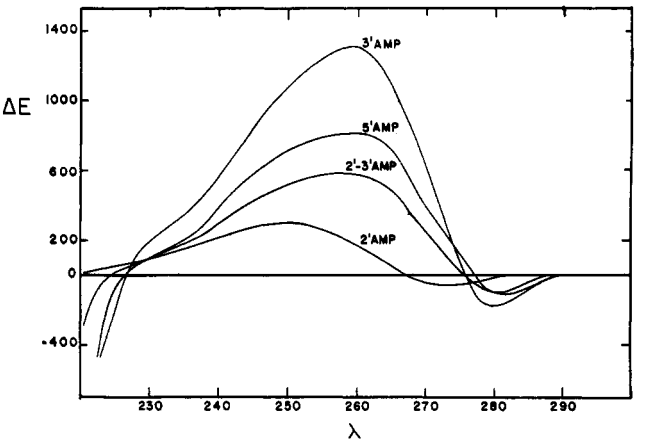

FIGURE 4: The interaction of cycloheptaamylose with various adenosine monophosphates: TSC buffer, 0.01 M cycloheptaamylose; 2':3'-AMP signifies adenosine 2':3'-cyclic phosphate.

The Effect of Variation of the Position of Phosphorylation of AMP. The following adenosine monophosphates were used in this experiment: 2'-AMP, 3'-AMP, adenosine 2':3'-cyclic phosphate (2':3'-AMP), and 5'-AMP. The spectral changes induced in these compounds by 0.01 M cycloheptaamylose in TSC are shown in Figure 4. In this series of compounds, $\Delta\epsilon$ is directly proportional to the distance of the phosphate group from the base on the ribose moiety.

The Effect of pH on the Interaction. The effect of pH on the interaction of cycloheptaamylose with a number of adenine- and hypoxanthine-containing compounds was also examined by the difference spectral technique, and the results are shown in Figure 5. Apparently, protonation of adenine residues reduces the interaction, while ionization of hypoxanthine has little or no effect. Unstacking of pApA

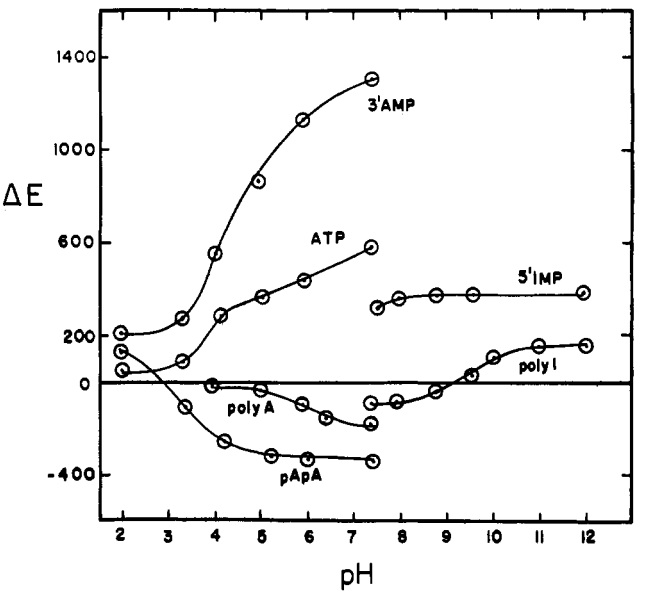

FIGURE 5: The effect of pH on cycloheptaamylose interaction with adenine- or hypoxanthine-containing compounds: cycloheptaamylose concentration, 0.01 M. Solutions were 0.1 M in NaCl and 0.01 M in the appropriate buffering compounds.

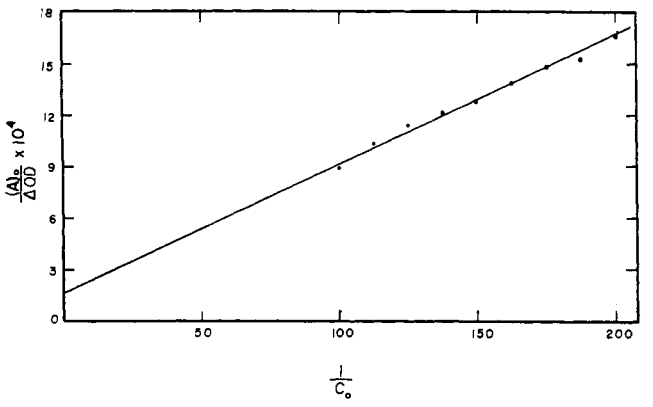

FIGURE 6: The determination of K_{eq} and $\Delta\epsilon_c$ for association of cycloheptaamylose and 3'-AMP. Abbreviations are defined in the text. Points represent the data at 260 mμ taken from difference spectra at nine cycloheptaamylose concentrations ranging from 0.01 to 0.005 M. The line drawn represents the least-squares fit to the points. Found: $K_{eq} = 22\,M^{-1}$, $\Delta\epsilon_c = 6.17 \times 10^3\,M^{-1}\,cm^{-1}$.

or poly I at extreme pH values causes the spectral shifts of these compounds to approach those of their respective mononucleotides.

Determination of the Equilibrium Constant for Association of Cycloheptaamylose and 3'-AMP. Since many other cyclodextrin inclusion complex systems are known to be weakly associated, the equilibrium constant for association of cycloheptaamylose and 3'-AMP was determined using a form of an equation derived by Colter *et al.* (1964).

$$\frac{(A)_0}{\Delta OD} = \frac{1}{(K_{eq})\,(C)_0\,(\Delta\epsilon_c)} + \frac{1}{\Delta\epsilon_c}$$

where $(A)_0$ is the initial concentration of AMP, K_{eq} is the equilibrium constant, $(C)_0$ is the initial concentration of cycloheptaamylose, and $\Delta\epsilon_c$ is the change in molar extinction coefficient on complete binding of 1 mole of AMP by cycloheptaamylose.

From this equation it can be seen that a plot of $(A)_0/\Delta OD$ *vs.* $1/(C)_0$ will have a slope of $1/(K_{eq}\Delta\epsilon_c)$ and an intercept of $1/\Delta\epsilon_c$, thereby allowing the determination of K_{eq} and $\Delta\epsilon_c$. For this determination, the difference spectra resulting from mixing a solution of AMP with cycloheptaamylose solutions ranging from 0.01 to 0.005 M were measured and the data at 260 mμ plotted as described. This plot is shown in Figure 6, where the line drawn represents a least-squares fit to the data. The values obtained are $K_{eq} = 22\ M^{-1}$, and $\Delta\epsilon_c = 6.17 \times 10^3\ M^{-1}\ cm^{-1}$.

The Effect of Polynucleotide Formation on Cycloheptaamylose-Induced Spectral Shifts. In order to determine the effect on cyclodextrin interaction of having the adenine or hypoxanthine bases in a single-stranded polymer, the difference spectra resulting from complexing the following compounds with cycloheptaamylose were measured: $(pA)_n$, n = 2 to 7, poly A, and poly I, all in TSC buffer.

Figure 7 summarizes the spectral results of complexing oligo or poly A with 0.01 M cycloheptaamylose in TSC buffer. The complete difference spectra for the trimer through the heptamer are not shown but fall within the envelope formed by poly A and pApA. The spectral shifts with oligo

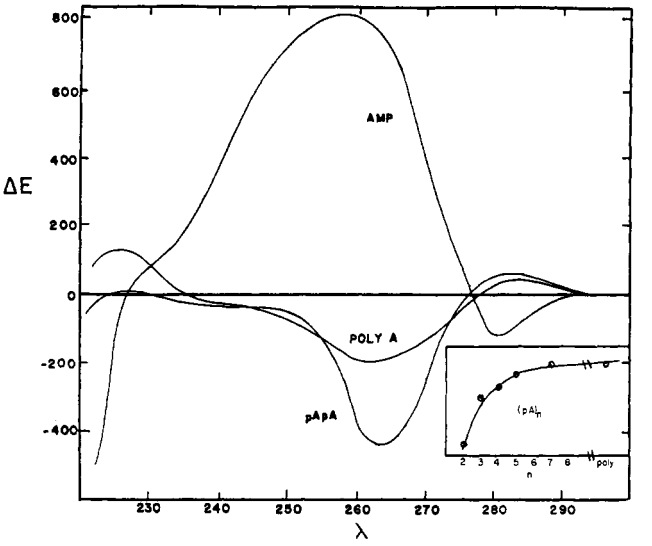

FIGURE 7: The effect of polymerization of adenylic residues on cycloheptaamylose-induced difference spectra: TSC buffer, 0.01 M cycloheptaamylose; inset: chain length n *vs.* $\Delta\epsilon_{263}$ for oligoadenylic acid. The ordinate of the inset is the same as for the overall figure. Complete difference spectra of the oligomers fall within the limits set by the pApA and poly A curves.

or poly A under these conditions are seen to be hyperchromic. Increasing chain length decreases the magnitude of the hyperchromic shift, as shown in the inset.

Figure 8 shows that the same effect, a reversal in the sign of the spectral shift, occurs on polymerization of IMP to poly I.

The effect of varying the bases neighboring adenine was examined in two ways. Figure 9 shows the difference spectra resulting from complexing 0.01 M cycloheptaamylose with four dinucleotides containing adenine. It is evident that the shapes of the difference spectra are dependent on the identity of the bases adjacent to adenine.

This is further illustrated in Figure 10, which shows the cycloheptaamylose-induced spectral changes with adenine-containing copolynucleotides compared to poly A. Again

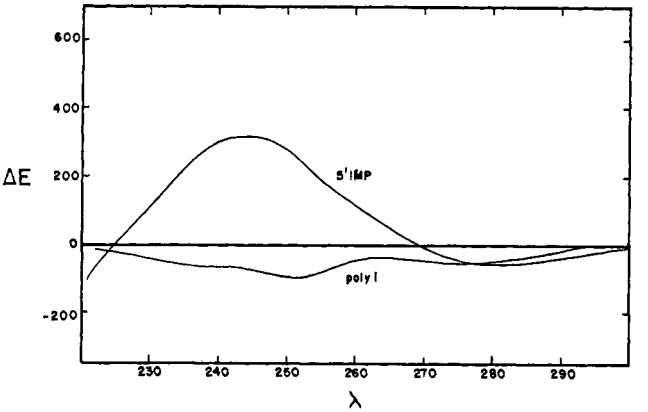

FIGURE 8: The effect of polymerization of inosinic acid residues on cycloheptaamylose-induced difference spectra: TSC buffer, 0.01 M cycloheptaamylose.

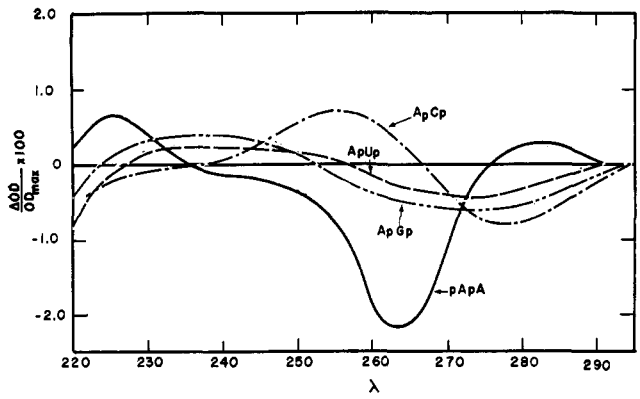

FIGURE 9: The cycloheptaamylose difference spectra of several adenine-containing dinucleotides: 0.01 M cycloheptaamylose in TSC buffer. Note that the ordinates in these and the remaining difference spectra are expressed as percent change in optical density relative to the maximum.

it can be seen that neighboring bases have an effect on the difference spectra.

Resistance to Cycloheptaamylose Complexing by Double- or Triple-Stranded Helical Polynucleotides. In order to be useful as a tool for detection of nonhelical regions in tRNA, cycloheptaamylose must not produce any spectral changes with helical complexes. If such changes were seen, it would be indicative of interaction with and/or denaturation of the helices by the cyclodextrin.

For this test, the difference spectra resulting from the interaction of 0.01 M cycloheptaamylose with the following helical complexes were measured: *E. coli* DNA, poly A:U, poly A:I, poly I:C, poly I:I:I (in 1 M NaCl; Haselkorn, 1959). In all cases, no spectral changes were detected. This means that on mixing the two solutions, the deviation from the base line was less than 0.002 optical density unit, the limit of accuracy for the spectrophotometer.

Characteristics of the tRNAs Studied. Table I lists several characteristics of the three tRNAs used in this work. In addition, Figure 11 shows the melting curves determined in TSC. Such broad curves, slightly multiphasic in character,

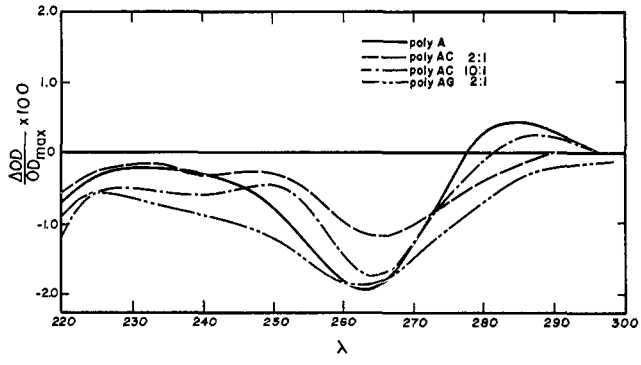

FIGURE 10: The cycloheptaamylose difference spectra of several adenine-containing copolynucleotides compared with poly A: 0.01 M cycloheptaamylose in TSC buffer. The numbers indicate the input ratios of nucleoside diphosphate substrates in the polynucleotide phosphorylase catalyzed preparation of these polymers.

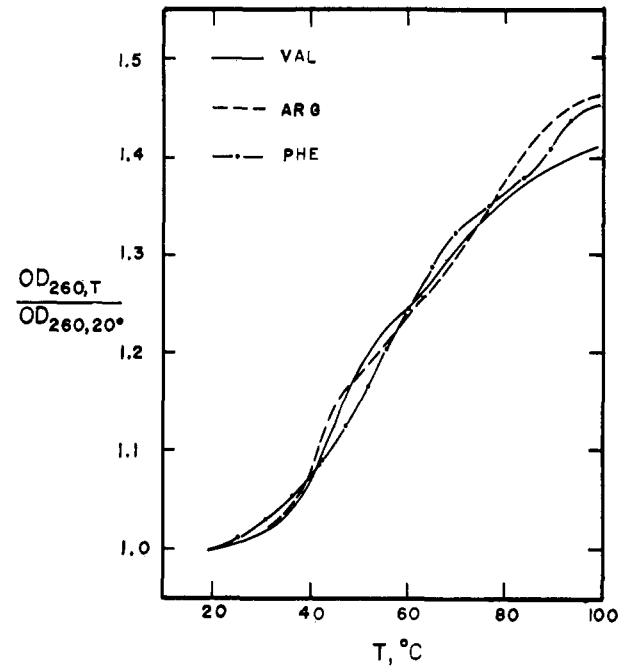

FIGURE 11: Melting curves of the three tRNAs studied. Determined in TSC buffer using the apparatus described in the text.

are typical of purified tRNAs in the absence of magnesium (Fresco *et al.*, 1963).

tRNA–Cycloheptaamylose Difference Spectra. Figure 12 shows the cycloheptaamylose-induced difference spectra of the alkaline digests of the three tRNAs. Note that these curves are quite similar to those for the adenine mononucleotides. It appears that the arginine tRNA may have a slightly higher adenine content than the other two.

Cycloheptaamylose-induced difference spectra of the three tRNAs and of their pancreatic RNase digests were measured in three different buffer solutions: 0.1 TSC, TSC, and TSC + 0.02 M magnesium acetate. These results are illustrated in Figures 13, 14, and 15. While the difference spectra of the RNase digests are not strongly affected by the varying solvent conditions, those of the intact tRNAs showed differing

TABLE I: Characteristics of the Three tRNAs Studied.

tRNA	% Purity	Codons Recognized	Optical Density Digested / Optical Density Intact: RNase	Optical Density Digested / Optical Density Intact: NaOH
E. coli Phe[a]	80[a]	UU,(U,C)[c]	1.32	1.39
Yeast Arg II[b]	80[b]	AG,(A,G)[d]	1.29	1.38
Yeast Val I[b]	70[b]	GU,(U,C,A)[d]	1.31	1.40

[a] Obtained from the Oak Ridge National Laboratory. [b] Cherayil and Bock (1965). [c] D. Soll, personal communication. [d] Soll *et al.* (1966).

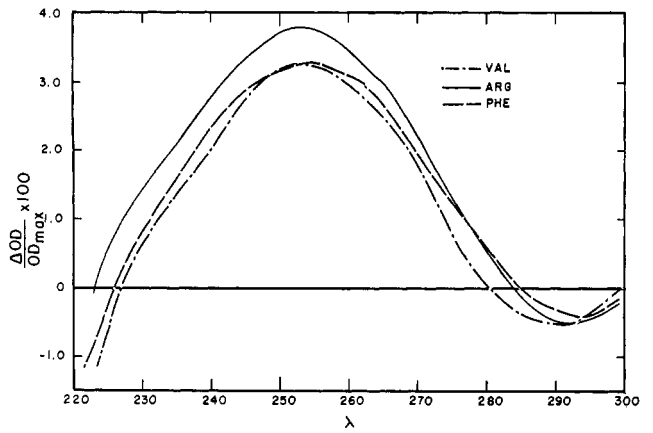

FIGURE 12: Cycloheptaamylose difference spectra of the NaOH digested tRNAs. NaOH hydrolysis was performed as described in the text. Samples were diluted into TSC buffer for spectral measurement. If necessary the pH of the diluted solutions was adjusted to 7.6 with HCl–cycloheptaamylose concentration, 0.01 M.

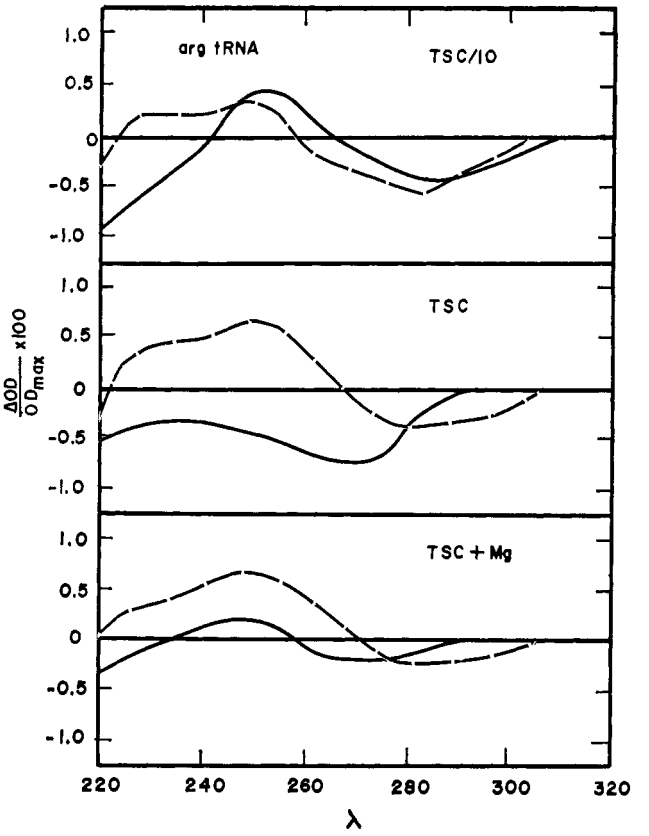

FIGURE 13: Cycloheptaamylose difference spectra of arginine tRNA: solid line, intact tRNA; dashed line, pancreatic RNase digest; 0.01 M cycloheptaamylose in the indicated buffer. TSC + Mg buffer contained 0.02 M magnesium acetate.

degrees of sensitivity to the solvent. The $tRNA^{Arg}$ was strongly affected, while the $tRNA^{Phe}$ was less so, and the difference spectrum of the $tRNA^{Val}$ was practically unaffected by changes in solvent conditions. This is emphasized in Figure 16 which is a replot of the difference spectra of the intact tRNAs from the three preceding figures shown together for purposes of comparison.

In all cases, the difference spectra for the intact tRNAs are much more similar to those of the RNase digests than to the NaOH digests shown in Figure 12.

Discussion

In an attempt to determine the rationale for the demonstrated base specificity, Corey–Pauling–Koltun models (Koltun, 1965) of the cyclodextrins (Figure 1) and mononucleotides were built and the fit of each of the bases into the cyclohexa- or cycloheptaamylose cavity was examined. While such a study has limitations, it complemented the spectral data in an encouraging manner.

All six of the bases examined were too large to fit into the cyclohexaamylose cavity. The pyrimidine bases C, U, and T appeared to be too small relative to the cycloheptaamylose cavity for significant stabilizing interactions to occur. Adenine and hypoxanthine fit closely into cycloheptaamylose, with numerous base–cyclodextrin contacts occurring but with no distortion of the cyclodextrin ring. On the other hand, the guanine base of GMP could be inserted into cycloheptaamylose only by distortion of the cyclodextrin ring.

The data in Figure 3 indicate that the presence of the ribose moiety lends additional stability to the adenine–cycloheptaamylose interaction. In addition, the presence of mono-, di-, or triphosphate groups on the ribose further stabilizes the complex. Again from examination of the models there are indications that multiple possibilities exist for hydrogen binding between the ribose–phosphate and the cyclodextrin. Also hydrophobic interactions between the 3- and 5-CH and 6-CH_2 groups of the cyclodextrin and similar groups of the ribose may occur. The ribose–phosphate limits the orientation of the base relative to the cavity in the complex.

The results in Figure 4 indicate yet another role for the ribose phosphate group in this interaction. In addition to stabilization and orientation as discussed above, phosphate groups apparently limit the depth of penetration of the base into the cyclodextrin cavity. Where the base and phosphate are immediately adjacent, as in 2′-AMP, studies of the models indicate that the phosphate hinders complex formation. As can be seen, the spectral change on mixing 2′-AMP with cycloheptaamylose is indeed much lower than those of the other monophosphates.

A comparison of the effect of pH on cycloheptaamylose interaction with AMP or IMP (Figure 5) reveals the following fact. Protonation of the adenine base of 3′-AMP (pK = 3.8) reduces the degree of interaction (*i.e.*, lowers $\Delta\epsilon$), while ionization of the enol group of IMP (pK = 8.9) has little or no effect. Although no ready explanation can be given for the difference in complex formation between a positively and negatively charged base, several suggestions may be made.

One possible explanation of this phenomenon might be differences in solvation between the two oppositely charged bases. Thoma and Stewart (1965) have implicated water structure in the cavity as a determinant of complexing ability, and it thus seems likely that solvated anions or cations would show differences in affinity for cyclodextrins.

Another possibility is that the fit between the base and cyclodextrin might be so critical that the small increase in

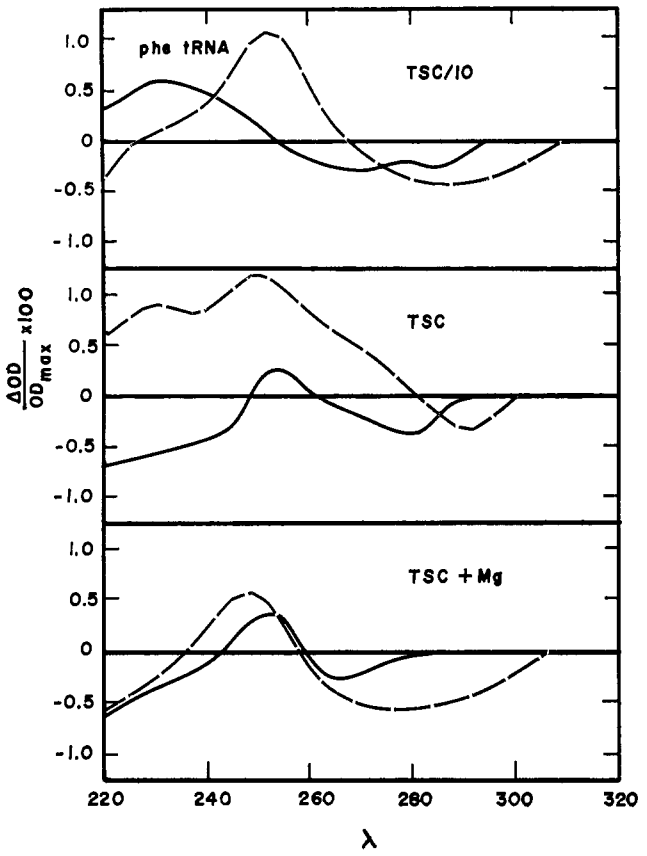

FIGURE 14: Cycloheptaamylose difference spectra of phenylalanine tRNA. See legend to Figure 13.

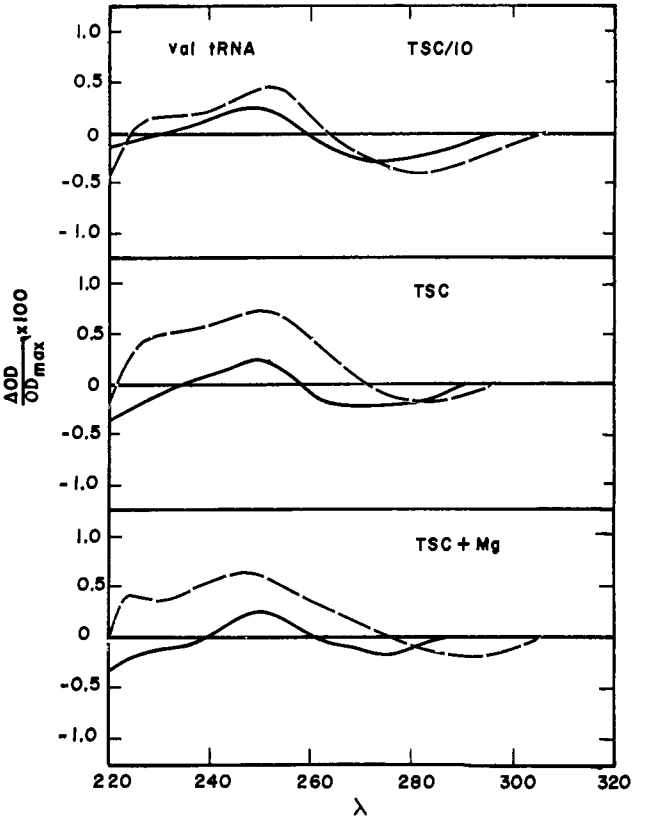

FIGURE 15: Cycloheptaamylose difference spectra of valine tRNA. See legend to Figure 13.

size upon protonation of adenine renders it too large, while removal of a proton from hypoxanthine still allows inclusion in the cavity.

The pH study again implicates the phosphate groups in stabilization of the complex, since in the pH range from 6 to 8 where no groups other than phosphate are being titrated, an effect is seen on the $\Delta\epsilon$'s of ATP, 3′-AMP, and IMP.

As the bases of pApA become positively charged and stacking interactions become disrupted by electrostatic repulsion, the cycloheptaamylose-induced $\Delta\epsilon$'s of pApA and 3′-AMP approach each other. This indicates that the protonated bases of these two compounds are in similar environments. Poly A, however, forms a helix at pH 5.5 (Rich *et al.*, 1961) and therefore the $\Delta\epsilon$'s merely go to zero, again demonstrating that bases in helices are resistant to cycloheptaamylose.

Poly I is somewhat similar to pApA since at high pH, the negatively charged bases repel each other and the spectral changes of poly I and IMP converge.

The results of the determination shown in Figure 6 give a value of 6.17×10^3 M^{-1} cm^{-1} for $\Delta\epsilon_0$, the decrease in molar absorption on complexing 3′-AMP and cycloheptaamylose. This compares with the decrease in molar absorption of 5.5×10^3 M^{-1} cm^{-1} resulting from polymerization of AMP to poly A. The value found for K_{eq} of the association was 22 M^{-1}. This corresponds to a $\Delta F°$ at 25° of about −1.8 kcal/mole. This value is of the same magnitude as the $\Delta F°$ for base stacking in poly A, found to be −1.1 kcal/mole (Brahms *et al.*, 1965).

Since π-orbital interactions between stacked bases in poly A give rise to changes in absorption and free energy similar to those resulting from cycloheptaamylose–AMP complexing, it is significant that Thoma and Stewart (1965) have described the interiors of cyclodextrin cavities as regions of high π electron density. This is a result of the distribution of the glycosidic oxygens around the interior of the molecule with their π orbitals orthogonal to the cylindrical axis of the cyclodextrin (Figure 1). It thus appears possible to have interaction between the π orbitals of the adenine and cyclodextrin.

Figure 7 demonstrates that the spectral changes induced in adenine residues are sensitive to the environment of the bases. Where the base is completely free as in AMP, a hypochromic change is seen on complexing with cycloheptaamylose. However when the bases are in a single-stranded oligomer or polymer, the opposite effect, a hyperchromic shift occurs, The same is true for hypoxanthine residues (Figure 8).

Base–base interaction causes considerable hypochromicity. This is evident in comparing the molar absorptions of AMP (15.4×10^3) and poly A (9.9×10^3) or of IMP (12.2×10^3) and poly I (10.2×10^3). It is not surprising then that the disruption of this interaction by insertion of the base into a cycloheptaamylose cavity results in a hyperchromic shift.

Such a shift is also found using mixed dinucleotides (Figure 9) or copolynucleotides containing adenine (Figure 10). Previous experiments had shown that cycloheptaamylose

does not interact with any base residues of these polymers other than adenine. Therefore the differences between the spectral changes of these compounds and those of pApA or poly A must be due to the fact that disruption of adenine–nonadenine stacking interactions occurs.

The finding that cycloheptaamylose does not interact with bases in helices completes the qualifications of this substance as a probe of base environment in nucleic acids. Stacked as they are in a helix, with hydrogen bonding in the center and the sugar phosphate chains winding around the outside, one would expect bases to be resistant to insertion into cycloheptaamylose.

We have shown that cycloheptaamylose interacts with adenine and hypoxanthine bases, producing spectral changes. If the bases are in an unstacked environment as in mononucleotides, pApA at acid pH values, or poly I at alkaline pH values, there is a hypochromic shift on interaction. If the bases are in a single-strand, stacked environment a hyperchromic shift is produced. And finally, if the bases are in a multistranded helix no interaction occurs.

It is obvious that cycloheptaamylose can be utilized in the study of tRNA structure. It has been proposed that tRNA consists of helical and nonhelical regions, the current most popular model being the "cloverleaf" structure put forth by Holley *et al.* (1965). This appears to be a reasonable model since it maximizes hydrogen bonding and creates universal spatial relationships between the aminoacyl-carrying 3′-terminal adenosine and the apparent anticodon triplet in each of several tRNAs whose base sequences have recently been determined (Holley *et al.*, 1965; Zachau *et al.*, 1966; Madison *et al.*, 1966; RajBhandary *et al.*, 1967).

To investigate the base environment in tRNA, model systems are needed to compare with the tRNAs. Pancreatic RNase was chosen to degrade tRNA into oligonucleotides consisting of oligo purines with 3′-terminal pyrimidines. The NaOH digestion would degrade the tRNAs to mononucleotides. Thus a comparison of the cycloheptaamylose difference spectra of the intact tRNAs with those of the digests will indicate if the nonhelical adenine bases of these tRNAs are in stacked or unstacked conformations.

Consideration of Figures 12 through 15 indicates that the nonhelical adenine bases of these three tRNAs are stacked. Although the difference spectra of the intact tRNAs are distinct from those of the RNase digests, they are similar in the sense that they do not have the strong positive lobe typical of free adenine bases. It is not until the tRNAs are completely hydrolyzed to mononucleotides with NaOH (Figure 12) that such strong hypochromic shifts are seen.

Base stacking in nonhelical tRNA loops may have been expected on the basis of previous studies of single-stranded oligo- and polynucleotides. In addition, recent model building studies by Fuller and Hodgson (1967) have demonstrated the feasibility and desirability of base stacking in the anticodon loop of tRNA. However we believe that this is a direct experimental demonstration that (adenine) base stacking occurs in tRNA.

The comparison of the difference spectra of the three tRNAs in Figure 16 reveals the effect of solvent conditions. Although they differ in low (1/10 TSC) and moderate (TSC) ionic strength buffers, addition of magnesium causes the difference spectral curves of the three tRNAs to approach each other in magnitude and shape. This is consistent with

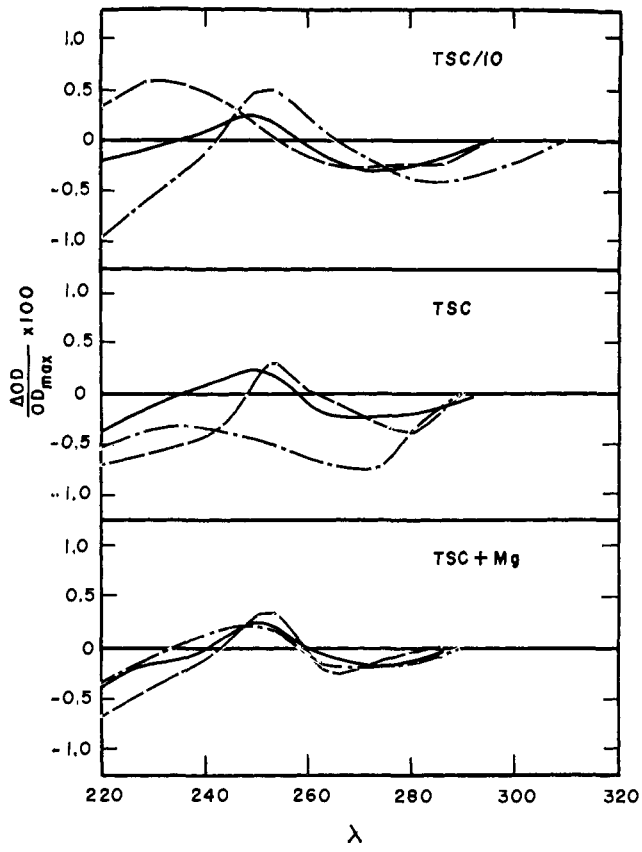

FIGURE 16: Comparison of the cycloheptaamylose difference spectra of the three tRNAs. These curves are replots of the data for the intact tRNAs from the three previous figures: (———) Val; (— —) Phe; (— -) Arg.

the view that all tRNAs have a similar biological conformation and that magnesium ions have a specific role in the maintenance of such a conformation (Fresco *et al.*, 1966).

Since the spectral shifts produced by cycloheptaamylose are due to interaction with only one or two base species (adenine or hypoxanthine), calculation of the per cent helix in tRNA from our data does not appear possible. Additional complications in such a calculation arise from attempting to choose a model system for 100% nonhelix. Although the RNase digests are certainly nonhelical, the dependence of $\Delta\epsilon$ on chain length as illustrated in Figure 7 rules out the use of such mixtures.

Bearing in mind these limitations however, we may attempt to rank the three tRNAs in order of base exposure to cycloheptaamylose. Examination of Figures 9 and 10 reveal certain wavelengths which may be useful in such an analysis. Note in these two figures that nearly all the curves intersect at 272 mμ. This wavelength thus appears to be insensitive to the identity of the bases neighboring adenine and spectral changes in this region depend only on the presence of an adenine base in a single-stranded region. We will use the magnitude of the negative spectral shifts at 272 mμ as an indication of "total" base exposure in the tRNAs.

Since the difference spectra in Figures 9 and 10 are sensitive to base composition at wavelengths other than 272 mμ, some indication of the base composition of the adenine-containing

TABLE II: Order of Base Exposure to Cycloheptaamylose. Interaction in Three tRNAs.

Buffer[a]	Base Exposure Measured[b]	Order of Base Exposure
TSC/10	Total	Phe = Val > Arg
	A	Phe > Val > Arg
	G,C	Arg > Phe = Val
TSC	Total	Arg > Phe = Val
	A	Arg > Val > Phe
	G,C	Arg = Phe > Val
TSC + Mg	Total	Arg = Phe = Val
	A	Phe > Arg > Val
	G,C	Arg = Val > Phe

[a] TSC is 0.01 M Tris–0.1 M Nacl, pH 7.6; TSC + Mg contains 0.02 M magnesium acetate. [b] Total measured at 272 mμ, A at 265 mμ, G,C at 280 mμ; see text for discussion.

nonhelical regions may be given. From these figures we have identified negative changes at 280 mμ as being indicative nonhelical adenines in (C + G)-rich regions. Negative spectral shifts at 265 mμ are apparently dependent on the presence of adenine in A-rich single-stranded regions.

Table II summarizes our attempts to rank the three tRNAs according to the exposure of their bases to cycloheptaamylose. In general it appears that yeast $tRNA_{II}^{Arg}$ has the greatest degree of base exposure followed by *E. coli* $tRNA^{Phe}$ and then yeast $tRNA_{I}^{Val}$. It should be noted that in the presence of magnesium ions, the apparent exposure of all the bases was quite low when compared with the other solvents.

References

Brahms, J., Michelson, A. M., and Van Holde, K. E. (1966), *J. Mol. Biol. 15*, 1467.

Cherayil, J. D., and Bock, R. M. (1965), *Biochemistry 4*, 1174.

Colter, A. K., Wang, S. S., Megerle, G. H., and Assip, P. S. (1964), *J. Amer. Chem. Soc. 86*, 3106.

Cramer, F., and Hettler, H. (1967), *Naturwissenschaften 54*, 625.

Englander, S. W., and Englander, J. J. (1965), *Proc. Nat. Acad. Sci. U. S. 53*, 370.

Fresco, J. R., Adams, A., Ascione, R., Henley, D., and Lindahl, T. (1966), *Cold Spring Harbor Symp. Quant. Biol. 31*, 527.

Fresco, J. R., Klotz, L. C., and Richards, E. G. (1963), *Cold Spring Harbor Symp. Quant. Biol. 28*, 83.

Fuller, W., and Hodgson, A. (1967), *Nature 215*, 817.

Haselkorn, R. (1959), Ph.D. Dissertation, Harvard University, Cambridge, Mass.

Holley, R. W., Apgar, J., Everett, G. A., Madison, J. F. Marquisee, M., Merrill, S. H., Penswick, J. R., and Zamir, A. (1965), *Science 147*, 1462.

Koltun, W. L. (1965), *Biopolymers 3*, 665.

Laskowski, M., Jr. (1966), *Fed. Proc., Fed. Amer. Soc. Exp. Biol. 25*, 20.

Litt, M., and Hancock, V. (1967), *Biochemistry 6*, 1848.

Madison, J. T., Everett, G. A., and Kung, H. (1966), *Science 153*, 531.

Marciello, R., and Zubay, G. (1964), *Biochem. Biophys. Res. Commun. 14*, 272.

Penniston, J. T., and Doty, P. M. (1963), *Biopolymers 1*, 145.

RajBhandary, U. L., Chang, S. M., Stuart, A., Faulkner, R. D., Hoskinson, R. H., and Khorana, H. G. (1967), *Proc. Nat. Acad. Sci. U. S. 57*, 751.

Rich, A., Davies, D. R., Crick, F. H. C., and Watson, J. D. (1961), *J. Mol. Biol. 3*, 71.

Seidel, H., and Cramer, F. (1965), *Biochim. Biophys. Acta 108*, 367.

Soll, D., Cherayil, J., Jones, D. S., Faulkner, R. D., Hampel, A., Bock, R. M., and Khorana, H. G. (1966), *Cold Spring Harbor Symp. Quant. Biol. 31*, 51.

Thoma, J. A., and Stewart, L. (1965), *in* Starch Chemistry and Technology, Vol I, Whistler, R. L., and Paschall, E. F., Ed., New York, N. Y., Academic, p 209.

Yankeelov, J. A., Jr. (1963), *Anal. Biochem. 5*, 2722.

Zachau, H., Dutting, D., and Feldman, M. (1966), *Angew. Chem. 78*, 393.